Intraseasonal Teleconnection between North American and Western North Pacific Monsoons with 20-day Time Scale

Xianan Jiang[1*], and Ngar-Cheung Lau[2]

[1]*Atmospheric and Oceanic Sciences Program, Princeton University, Princeton, NJ*
[2]*NOAA/Geophysical Fluid Dynamics Laboratory, Princeton University, Princeton, NJ*

1. Introduction

The North American monsoon (NAM) exerts profound societal and economic impacts on the region of northwestern Mexico and the southwestern U.S. As one of the active components of the climate system over North America during the warm season, the NAM plays an important role in the climate variability in that region. A better understanding of this phenomenon is essential for improving our skill in making predictions of the weather and climate over North America.

While the active/break cycles of summer monsoon over the Asian continent have been intensively investigated during the past decades, studies on the subseasonal variability (SSV) of the NAM remain limited. Recently, Lorenz and Hartmann (2006) proposed that the eastward propagating Madden-Julian Oscillation (MJO) along the equator could exert a significant impact on ISV of rainfall over the NAM region by modulating activities of synoptic systems over the eastern equatorial Pacific, including easterly waves, tropical storms, and surge events over the GoC. Higgins et al. (2004), however, indicated that the moisture surges over the Gulf of California (GoC) may not necessarily lead to enhanced rainfall over the NAM region. Furthermore, Mo and Nogues-Paegle (2005) noted only a weak influence of the MJO on summertime rainfall over the southwestern U.S. The dominant mode that affects active and break periods of rainfall over the southwestern U.S. has a time scale of 20-28 d (Mo, 2000). A characteristic time scale of about 20 d for rainfall variability over the southwestern U.S. has also been reported by Mullen et al. (1998) and Kiladis and Hall-McKim (2004). Thus, more efforts are needed to improve our understanding of the physical mechanisms responsible for ISV of NAM rainfall.

2. Data and approach

The primary observational dataset for this study is the North American regional reanalysis (NARR; Mesinger et al. 2006). Variables include daily averaged data for precipitation rate, wind, geopotential height and specific humidity at 29 pressure levels. Same variables based on ERA-40 reanalyses and NOAA OLR are also examined in order to determine the linkage of the global circulation pattern to ISV of rainfall over the NAM region.

After removing the mean seasonal cycle in the raw data, a low-pass time filter is applied to various data fields to exclude synoptic-scale activities with periods of less than 8 d. Thus the contributions of tropical storms and easterly waves to the time series being analyzed are eliminated. The results reported in the following are based on the filtered time series extending from June 21 to August 31 of each year in the 1979-2001 period.

3. Evolution of atmospheric features associated with ISV of NAM rainfall

a. NAM rainfall index

Since the rainfall field in the NARR largely relies on gauge observations over land, in view of the density of gauge observations in the NAM region, one would expect that NARR rainfall data are more accurate in the U.S. than in Mexico. Thus, the area over Arizona and New Mexico (AZNM hereafter) between 32-36ºN and 112-107ºW (see purple rectangular box in upper-left panel in Fig. 1) is chosen for computation of the areal average

Correspondence to: Correspondence to: Xianan Jiang, Jet Propulsion Laboratory, MS 183-501, California Institute of Technology, 4800 Oak Grove Drive, Pasadena, CA 91109; E-mail: xianan@caltech.edu.

rainfall index. The selection of this domain is nearly identical to that adopted in previous studies (e.g., Higgins et al. 2004; Kiladis and Hall-McKim 2004).

b. Local features associated with ISV of NAM

Figure 1 shows the regression charts of rainfall at individual grid-points versus the daily AZNM rainfall index at various lags. The results illustrate that the rainfall center over AZNM at day 0 can be traced back to the rainfall over the Gulf of Mexico (GoM) and tropical eastern Pacific more than one week earlier. On day -10, the heaviest rainfall is located over coastal regions of Mexico, with one center in the western GoM and another over the eastern edge of the tropical Pacific. In the ensuing days (day -8 to day -4), wet conditions still prevail over eastern Mexico; whereas enhanced rainfall spread northwestward along the slope of SM Occidental. On day -4, the rainfall maximum along the SM Occidental arrives at northwestern Mexico, just to the south of Arizona. Thereafter, the rainfall center further migrates northward into the AZNM region. After it arrives at AZNM on day 0, the rainfall decreases markedly and eventually dissipates over the southwestern U.S. on day 4. It is interesting to note that a negative rainfall anomaly emerges over the coastal Mexico along 20ºN on day 2. Comparison among the individual panels in Fig. 1 indicates that the rainfall pattern on day 4 and that on days -8 or -6 represent two opposite phases of the rainfall evolution, thus suggesting that the rainfall variation over the NAM region has a cyclical character, with an intraseasonal time scale of about 20 days. This result is in agreement with previous studies on the dominant period of NAM variability (e.g., Mullen et al. 1998; Mo 2000).

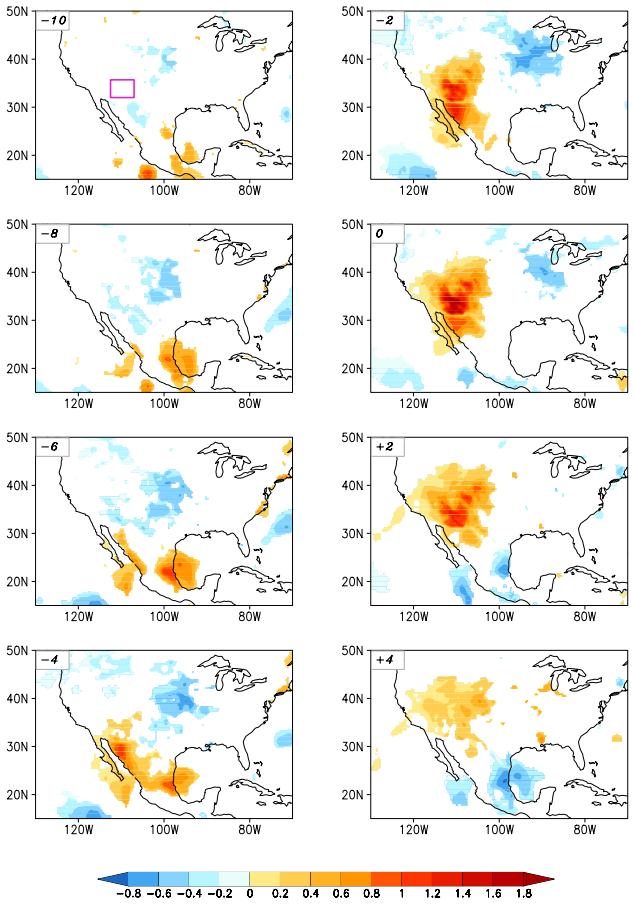

Fig. 1 Distributions of regression coefficients of 8-d low-pass filtered rainfall versus the standardized AZNM rainfall index at time lags ranging from day -10 to day +4, as computed for the NAM season (June 21~Aug. 31) during the 1979-2001 period. Only regression coefficients surpassing the 95% significance level are plotted (units: mm d^{-1}).

To gain a better understanding of the evolution of rainfall features described above, the regional-scale circulation pattern over North America associated with rainfall variability over AZNM is further analyzed using regression maps of geopotential height and wind vectors at different vertical levels and at time lags ranging from day -8 to day 2. In Fig. 2, these charts for 200hPa, 500hPa and 850hPa are displayed in the left, middle and right columns, respectively; and the results for individual lags are arranged vertically within each column.

At 200hPa, about one week prior to the rainfall peak over AZNM (day -8 to day -6), an anticyclonic circulation center appears over the western U.S. at 40ºN. This feature remains quasi-stationary between day -6 and day -2. At the same time, an intensifying cyclonic vortex travels westward over the GoM. After day -2, as the rainfall over AZNM attains maximum intensity, the anticyclonic center over the western U.S. starts to move eastward. The subtropical cyclonic vortex over the GoM quickly extends westward from day -2 to day 0. Thereafter, this feature gains further strength as it propagates northwestward over the Pacific Ocean off Baja California.

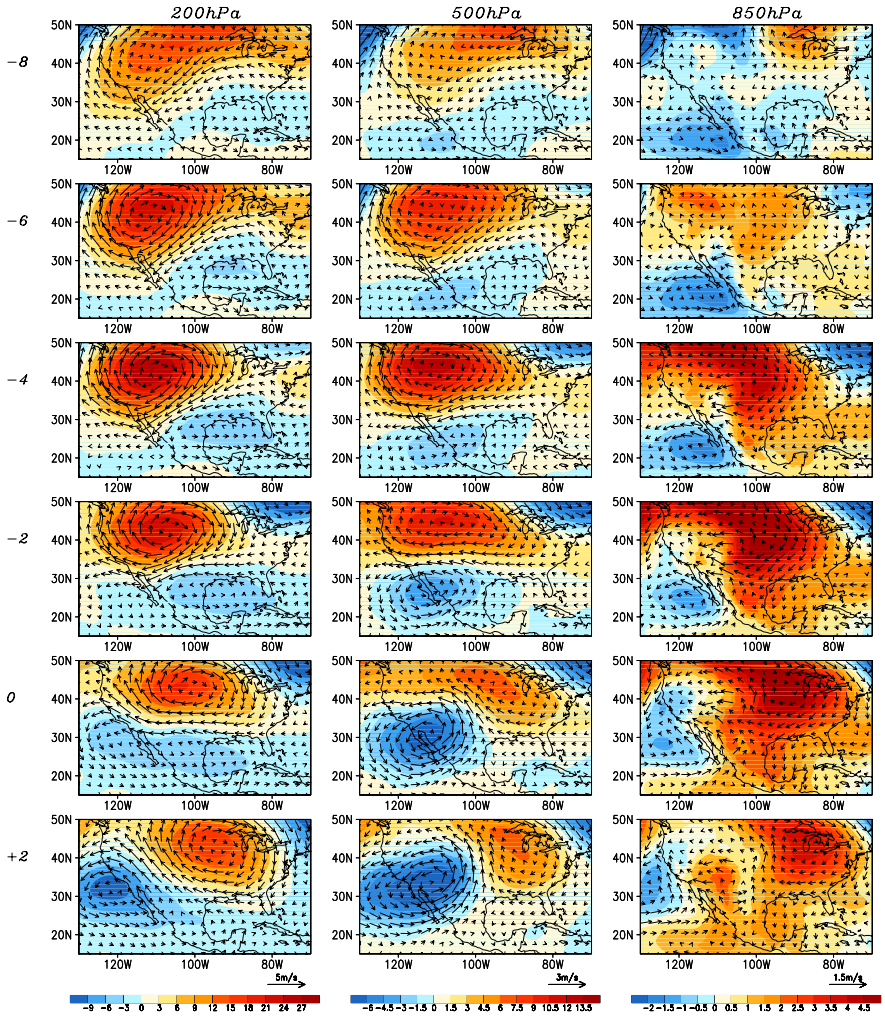

Fig. 2 Distributions of the regression coefficients of the 8-d low-pass filtered geopotential height (shading) and wind vectors (arrows) versus the standardized AZNM rainfall index at time lags ranging from day -8 to day 2, for the (left) 200hPa, (middle) 500hPa and (right) 850hPa levels. The scales for the geopotential height (units: m) and wind vectors for each pressure level are indicated at the bottom of the respective column. All computations are based on NARR data.

Inspection of the circulation patterns at 500hPa and 850hPa illustrates that the mid-latitude high over the U.S. exhibits an almost equivalent barotropic structure, with a slight westward tilt with increasing height in the lower troposphere. The subtropical cyclone feature, however, displays a complicated vertical structure. While the westward movement of the low center from Florida to Mexico is evident at 200hPa, the low center at 500hPa is mainly situated over western Mexico/eastern Pacific. At 850hPa, the negative height perturbations in the subtropics are mainly confined above the ocean surface of the eastern Pacific and western GoM. From day -8 to day -2, the low center over western GoM gradually diminishes. After day -2, the vortex over the eastern Pacific undergoes northwestward movement along the coastal region off California as detected at other vertical levels. The behavior of the low-level wind and height pattern is consistent with the rainfall evolution features shown in Fig. 1, suggesting that the low-level circulation may play a pivotal role in modulating the rainfall evolution over ANZM. (Further analyses suggest that the enhancement of rainfall over AZNM is largely consistent with moisture convergence brought by low-level circulation.)

Particularly noteworthy is the prevalence of southeasterly flow at 850hPa along GoC on day 0, when maximum rainfall occurs over AZNM. This low-level wind anomaly is associated with the cyclonic circulation over the eastern Pacific and anticyclonic circulation over the continental U.S, and markedly resembles the synoptic situation during typical “gulf surge” events (e.g., Stensrud et al. 1997). The same characteristic low-level circulation pattern at day 0 is reminiscent of the setting favoring the “wet surge” events over southwestern U.S., as illustrated by Higgins et al. (2004).

4. Global teleconnections

a. Geopotential height and OLR patterns

Figure 3 shows regression patterns of 850hPa geopotential height and wind fields versus the standardized AZNM rainfall index. These charts are analogous to those presented in the right column of Fig. 2, except that they are based on ERA-40 reanalysis data with global coverage. The most prominent feature is the arch-shaped trans-Pacific wave-train connecting circulation centers over the WNP with those over the eastern subtropical Pacific/North America. The low-level cyclonic center over the eastern Pacific Ocean near 120°W, which plays an essential role in modulating rainfall variation over the NAM region as previously noted, is apparently one component of this trans-Pacific wave-train. Moreover, the northwestward movement of this vortex over eastern Pacific off California is associated with the overall counterclockwise propagation of the individual centers along the entire length of the wave-train spanning over the North Pacific. On day -6, a prominent anticyclonic center is located over the Philippine and South China Seas, i.e., in the westernmost part of the trans-Pacific wave-train. In conjunction with the overall counterclockwise propagation of the perturbations embedded in this wave-train, this anticyclonic center moves southwestward to South China Sea and the Indo-China Peninsula.

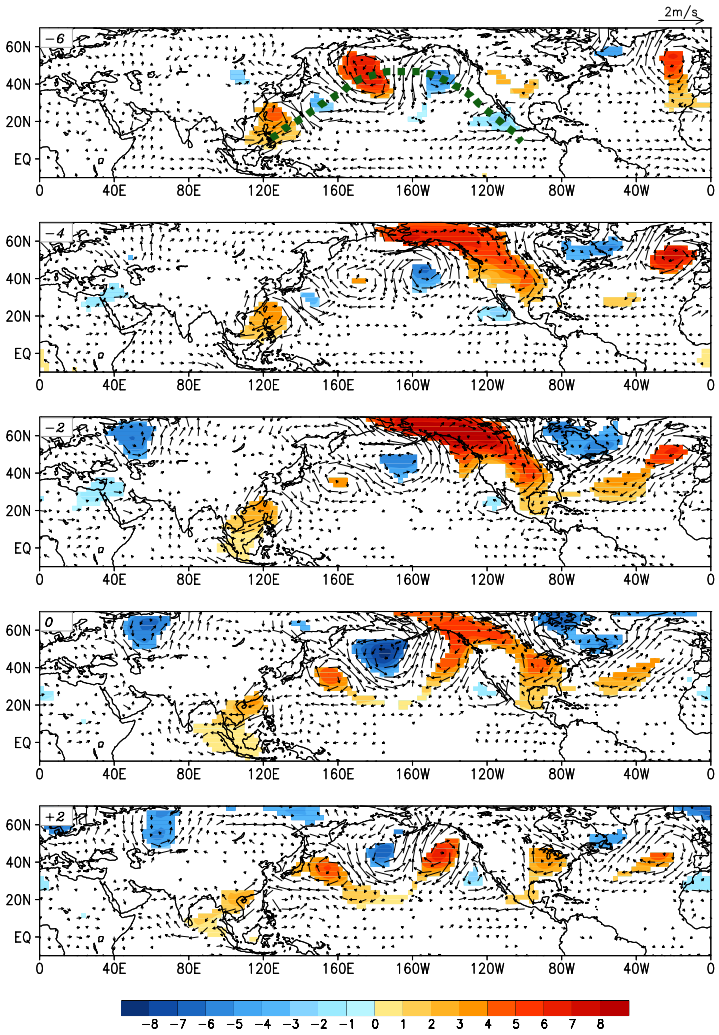

Fig. 3 Distributions of regression coefficients of 8-d low-pass filtered 850hPa geopotential height (shading; units: m) and wind vectors (arrows; see scale at upper right) versus the standardized AZNM rainfall index at time lags ranging from day -6 to day 2. Only geopotential height signals surpassing the 90% significance level are plotted. Wind vectors smaller than 0.25 ms^{-1} are omitted. The height and wind data are obtained from the ERA-40 reanalyses. The green dashed line in the top panel indicates the axis of the trans-Pacific wave-train.

Comparison between Fig. 3 and its upper-tropospheric counterpart (figure not shown) indicates that the circulation features along the North Pacific segment of the wave-train exhibit an almost equivalent barotropic structure. In contrast, the anomalies have a distinct baroclinic character near the Philippine Sea, with a high center at low-level being overlain by a low center at upper-level. Such differences in the vertical structure in various portions of the wave-train is clearly evident in Fig. 4, which shows the cross-section of geopotential height perturbations along the wave-train axis on day -6 (see green dashed line in the upper panel of Fig. 3). A predominantly barotropic structure prevails at most locations, except those over the WNP near 120°E. The baroclinic character over the WNP is suggestive of the important role of latent heat release associated with convection in that region; whereas the equivalent barotropic structure in the remaining portion of the wave-train is the signature of Rossby wave energy dispersion. In view of the placement of the baroclinic structure near the western edge of the wave-train, this wave-train is likely a response to the convective activity over the WNP.

In order to highlight the convection activities in various regions that are associated with ISV of the NAM rainfall, global lag-regression patterns have also been constructed using the OLR dataset. The results reveal that the trans-Pacific wave-train, as previously identified using geopotential height data, is also associated with

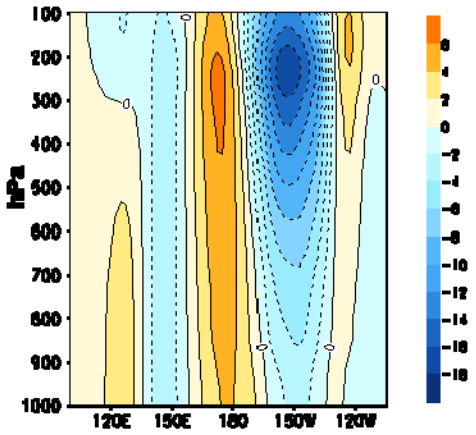

Fig. 4 Vertical cross-section of the regression coefficients of 8-d low-pass filtered geopotential height versus the standardized AZNM rainfall index at the time lag of day -6 (units: m). The abscissa corresponds to the axis of the Pacific wave-train, as denoted by the green dashed line in the top panel of Fig. 6. The height data are obtained from the ERA-40 reanalyses.

distinct perturbations in convective activity (figure not shown). The alternate high (low) centers along the wave-train in Fig. 3 are generally collocated with suppressed (enhanced) convection, especially over the tropical and subtropical regions. In particular, the center of suppressed convection over the WNP associated with local high anomaly also moves southwestward with time, following the path taken by the high anomaly in that region (see Fig. 3).

b. Wave-activity flux

The nature of energy propagation along the wave-train is further diagnosed using the wave-activity flux vector (Takaya and Nakamura 2001). Figure 5 shows the regression patterns for wave-activity flux (vectors) and its divergence (shading) at 850hPa on day -6. The summer mean zonal wind at this level is also depicted using contours. The pattern of wave-activity flux indicates energy transport from the WNP to North America along the wave-train axis (cf. Fig. 3). The energy source that maintains the low-level wave-train is located over the WNP monsoon region near the Philippine Sea, where divergence of wave-activity flux occurs. Positive anomalies in geopotential height (Fig. 3) prevail over this region on day -6. Thus, the results in Fig. 5 provide further evidence on the key role of convective activities over the WNP monsoon region in generating and sustaining the trans-Pacific wave-train. It is also worth noting that the arch-shaped pattern of the wave-activity fluxes over the North Pacific is collocated with strong mean westerlies associated with the climatological subtropical high residing over the western Pacific in the lower troposphere. This mean circulation may serve as a wave guide for the Rossby wave train.

5. Summary and discussion

Based on a recently released, high-resolution reanalysis dataset for the North American region, the ISV with a time-scale of about 20 d of the NAM is examined. The rainfall signals associated with this phenomenon first emerge near the Gulf of Mexico and eastern Pacific at about 20ºN. They subsequently migrate to the southwestern U.S. along the slope of the Sierra Madre Occidental. The rainfall quickly dissipates upon arrival at the desert region of AZNM. The enhanced rainfall over AZNM is accompanied by strong southeasterly low-level flow along the Gulf of California. This pattern bears strong resemblance to the circulation related to "gulf surge" events, as documented by many studies. The southeasterly flow is associated with an anomalous low vortex over the subtropical eastern Pacific Ocean off California, and a mid-latitude anticyclone over the central U.S in the lower troposphere. This flow pattern is in broad agreement with that favoring the "wet surges" over the southwestern U.S.

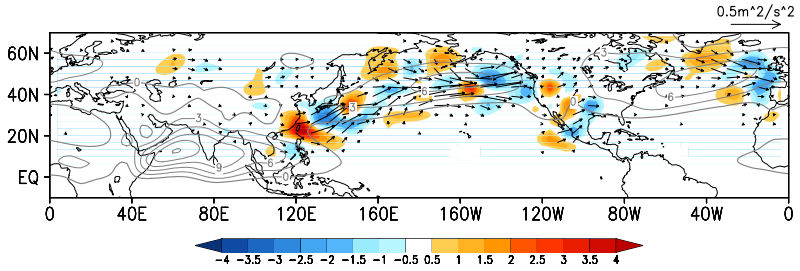

Fig. 5 Distributions of the regression coefficients of 8-d low-pass filtered wave-activity flux (arrows) and wave-activity flux divergence (shading; units: 10^{-7} ms^{-2}) at 850hPa versus the AZNM rainfall index on day -6, and summer mean zonal wind component (contours; units: ms^{-1}; only positive values indicating westerlies are plotted). Data for the wave-activity flux and zonal wind are obtained from the ERA-40 reanalyses.

It is further demonstrated that the aforementioned low-level circulations associated with ISV of the NAM are part of a prominent trans-Pacific wave-train extending from the WNP to the Eastern Pacific/North America along a "great circle" path. The circulation anomalies along the axis of this wave-train exhibit a barotropic vertical structure over most regions outside of the WNP, and a baroclinic structure over the WNP, thus suggesting the important role of convective activities over the WNP in sustaining this wave-train. This inference is further substantiated by an analysis of the pattern of wave activity-flux vectors. Variations in the WNP convection are correlated with the ISV of the monsoons in both North American and East Asian (EA)/WNP sectors. These relationships lead to notable teleconnections between NAM and the EA/WNP monsoon on 20-day time scales.

It is worth noting that the ISV with a time scale of about 20 d associated with EA/WNP monsoon has also been documented in many previous studies. Of particular interest are the investigations of Fukutomi and Yasunari (1999, 2002), who examined the spatial and temporal evolution of the 10-25 d intraseasonal variations over the WNP during June-August by using the OLR over 10-20ºN and 100-120ºE as an index for composite analysis. Their results are very similar to those illustrated in the present study, including a distinct wave-train extending from the WNP to North Pacific; transition from a baroclinic structure over WNP to an equivalent barotropic structure farther downstream; and southwestward movement of the low-level circulation and convective center over WNP. Note that the 8-day low pass filtered data employed in the present study has not been subjected to time filtering with a specific intraseasonal time scale. Hence the agreement between the findings in our study and those in previous works on ISV in the Asian sector offers independent substantiation of the strong linkage between the WNP/EA monsoon and the NAM on intraseasonal time scales.

References

Fukutomi, Y., and T. Yasunari, 1999: 10-25-day intraseasonal variations of convection and circulation over East Asia and western North Pacific during early summer. J. Meteor. Soc. Japan, 77, 753-769.

_____, and T. Yasunari, 2002: Tropical-extratropical interaction associated with the 10-25-day oscillation over the Western Pacific during the northern summer. J. Meteor. Soc. Japan, 80, 311-331.

Higgins, R. W., W. Shi, and C. Hain, 2004: Relationships between Gulf of California moisture surges and precipitation in the southwestern United States. J. Climate, 17, 2983-2997.

Kiladis, G. N., and E. A. Hall-McKim, 2004: Intraseasonal modulation of precipitation over the North American monsoon region. Proc. 15th Symposium on Global Change and Climate Variations, Amer. Meteor. Soc., Seattle, WA. 10-16 January 2004.

Lorenz, D. J., and D. L. Hartmann, 2006: The Effect of the MJO on the North American Monsoon. J. Climate, 19, 333–343.

Mesinger, F., and coauthors, 2006: North American Regional Reanalysis. Bull Amer. Meteor. Soc., 87, 343-360.

Mo, K. C., 2000: Intraseasonal modulation of summer precipitation over North America. Mon. Wea. Rev., 128, 1490-1505.

_____, and J. Nogues-Paegle, 2005: Pan-America. Intraseasonal Variability in the Atmosphere-Ocean System. K. M. Lau and D. E. Waliser, Ed., Praxis, 95-124.

Mullen, S. L., J. T. Schmitz, and N. O. Renno, 1998: Intraseasonal variability of the summer monsoon over southeast Arizona. Mon. Wea. Rev., 126, 3016-3035.

Stensrud, D. J., R. L. Gall, and M. K. Norquist, 1997: Surges over the Gulf of California during the Mexican monsoon. Mon. Wea. Rev., 125, 417-437.

Takaya K., and H. Nakamura, 2001: A formulation of a phase-independent wave-activity flux for stationary and migratory quasigeostrophic eddies on a zonally varying basic flow. J. Atmos. Sci., 58, 608–627.